

## Coherent Optical Photons from Shock Waves in Crystals

Evan J. Reed,<sup>1,2,\*</sup> Marin Soljačić,<sup>1</sup> Richard Gee,<sup>2</sup> and J. D. Joannopoulos<sup>1</sup>

<sup>1</sup>Center for Materials Science and Engineering and Research Laboratory of Electronics, Massachusetts Institute of Technology, Cambridge, Massachusetts 02139, USA

<sup>2</sup>Lawrence Livermore National Laboratory, Livermore, California 94551, USA

(Received 24 August 2005; published 11 January 2006)

We predict that coherent electromagnetic radiation in the 1–100 THz frequency range can be generated in crystalline materials when subject to a shock wave or solitonlike propagating excitation. To our knowledge, this phenomenon represents a fundamentally new form of coherent optical radiation source that is distinct from lasers and free-electron lasers. The radiation is generated by the synchronized motion of large numbers of atoms when a shock wave propagates through a crystal. General analytical theory and NaCl molecular dynamics simulations demonstrate coherence lengths on the order of mm (around 20 THz) and potentially greater. The emission frequencies are determined by the shock speed and the lattice constants of the crystal and can potentially be used to determine atomic-scale properties of the shocked material.

DOI: 10.1103/PhysRevLett.96.013904

PACS numbers: 42.72.–g, 47.40.Nm

The invention of lasers in 1958 made possible a staggeringly wide range of applications. The key characteristic of lasers that enables many of these applications is the fact that they are sources of *coherent* light. Almost 50 years later, very few distinct ways to generate coherent light have been realized. These include “traditional” lasers based on stimulated emission and free-electron lasers [1], each with its own unique practical advantages and disadvantages. This work presents what we believe is a new source of coherent optical radiation that is fundamentally distinct from lasers and free-electron lasers.

In this work, we ask what kind of electromagnetic radiation is produced if one takes a dielectric crystalline material [it can be almost any crystal, e.g., kitchen salt (NaCl)] and generates a mechanical shock wave inside the crystal. It might be expected that only incoherent photons and sparks will be observed emerging from the crystal. Remarkably, our analytical theory and computational experiments predict that weak yet measurable *coherent* light can be observed emerging from the crystal, typically in the range 1–100 THz. The radiation is generated by an oscillating dipolelike material polarization resulting from the synchronized motion of large numbers of atoms induced by a planar shock wave propagating through the crystalline lattice. The periodicity of the crystalline lattice is the origin of the coherence of emitted radiation rather than the “coherence” of the source generating the shock wave.

This effect is predicted to be observable in a wide variety of material systems under realizable shock wave conditions. In practice, shock waves in materials are typically generated using sources like gun-driven projectile mechanical impacts (see, e.g., Ref. [2]) or ablation of materials with laser pulses (see, e.g., Ref. [3]). In this work, we consider shock waves in NaCl. Some experiments on shocked single NaCl crystals have been reported [4]. To our knowledge, coherent emission has never been observed because a shocked crystal is not an obvious system to

discover (and hence look for) coherent radiation, and the radiation is in a portion of the electromagnetic spectrum that is usually not observed in such experiments.

*Analytical theory.*—As a shock propagates through a polarizable crystal, a change in polarization can be induced that yields a time-dependent polarization current (even in materials with no static polarization). While it is not surprising that radiation should be emitted from the polarization currents induced by the shock, it is unexpected that this emission should be of a coherent nature. The coherent property of the radiation is the subject of this work. The frequencies of the polarization current are associated with the temporal period of the shock propagating through a single lattice unit of the crystal. The periodicity of the crystal lattice is the true origin of the coherent emission.

In this section we use an analytical approach to demonstrate the coherent nature of the emitted radiation. To represent the material, a polarizable element  $P_n(t)$  that exists on each lattice point  $n$  located at  $x = na$  obeys the equation,

$$\frac{d^2 P_n(t)}{dt^2} = \mu_n(t) E_n(t) - \Omega_n(t)^2 P_n(t) - f_n(t) - \gamma(t) \frac{dP_n(t)}{dt}. \quad (1)$$

Here,  $\mu_n(t)$  is a polarizability-related parameter,  $\Omega_n(t)$  is the resonant frequency of the  $n$ th polarizable element, and  $\gamma(t)$  is an absorption term. The term  $f_n(t)$  represents coupling to the shock wave and is a forcing term that generates shock-induced changes in polarization.  $\Omega_n$  is the local transverse optical mode frequency ( $\omega_T$ ) ranging from  $10^{13} \text{ s}^{-1}$  for phonons in ionic crystals to  $10^{15} \text{ s}^{-1}$  and higher for electronic excitations. Equation (1) can model many polarizable materials when combined with Maxwell’s equations. In the case where  $\Omega_n(t)$  and  $\mu_n(t)$  are time independent and  $f_n = 0$ , Eq. (1) produces the usual polariton dispersion relation [5]. For simplicity in this section, we consider shock amplitudes sufficiently

weak to preclude disordering of the crystal lattice, typically with strains on the order of 0.01.

To determine emission characteristics of this shocked polarizable material, we perform a symmetry analysis of the classical equations of motion of the system. There exists a time and space translational invariance of this system that gives rise to a Bloch-like property for the fields. Define a space and time translation operator  $\hat{T}_m$  such that  $\hat{T}_m g_n(t) \equiv g_{n-m}(t - m\frac{a}{v_s})$ . In the shock wave, suppose that the polarizable elements have the property that  $\hat{T}_m \mu_n(t) = \mu_n(t)$ ,  $\hat{T}_m \Omega_n(t) = \Omega_n(t)$ ,  $\hat{T}_m f_n(t) = f_n(t)$ , and  $\hat{T}_m \gamma_n(t) = \gamma_n(t)$ . Comparison of the fields in Eq. (1) and Maxwell's equations with and without the application of  $\hat{T}_m$  leads to the result that the electric field  $E$  must be of the form

$$E = \sum_k e^{ik(x-v_s t)} \sum_\ell E'_{k,\ell} e^{-2\pi i \ell (v_s/a)t}, \quad (2)$$

where  $\ell$  is an integer,  $k$  is a wave vector, and  $H$  has a similar form. The Bloch-like property of the fields yields a condition on the radiation emitted by the shock wave. Possible frequencies in the fields in Eq. (2) are

$$\omega_1 = k_1 v_s + 2\pi \ell \frac{v_s}{a}, \quad (3)$$

where subscript 1 denotes the output radiation. Possible emission frequencies into the preshock and postshock materials are those for which Eq. (3) and  $\omega(k_1)$  for the preshock and postshock materials have common solutions, respectively. The emission frequencies for  $\ell \neq 0$  are highly anomalous since  $\frac{2\pi}{a} \gg k_1$ . Since the lattice constant  $a$  is typically several orders of magnitude smaller than the wavelength of optical light, these frequencies for  $\ell \neq 0$  are larger than a typical Doppler shift ( $k_1 v_s$ ) by several orders of magnitude. The confinement of the emitted radiation to discrete frequencies demonstrates the coherent nature in this model.

We have performed a quantum field theory analysis of this system (details in Ref. [6]) that yields the same emitted frequencies as the classical case, given in Eq. (3). While one might think that stimulated emission should be necessary for coherent emission, stimulated emission is not required when the system is coherently prepared as in, for example, so-called correlated spontaneous emission "lasers" [7].

*Computational experiments.*—In this section, we numerically explore the light generated by a shocked polarizable material by performing molecular dynamics (MD) simulations of shock waves (see, for example, Ref. [8]) propagating through crystalline NaCl. Such commonly utilized simulations solve the classical equations of motion for atoms subject to an empirically constructed interaction potential and incorporate thermal effects and deformation of the crystal lattice. In these calculations, planar shock waves are generated within 3D computational cells of perfectly crystalline atoms with cross section  $17 \times 17 \text{ nm}^2$

and length in the shock propagation direction ranging from 158 to 235 nm [ $(2-3) \times 10^6$  atoms] at  $T = 4.2 \text{ K}$  by constraining atoms at one edge of the long dimension of the computational cell to move into the cell like a piston (representing the mechanical driving force or object that generates the shock). Because of periodic boundary conditions in the directions transverse to the propagation direction, an infinitely planar shock propagates away from the constrained atoms into the cell that is oriented along either the [111] or [100] directions of NaCl. We have performed simulations with computational cell cross sections of up to  $135 \times 135 \text{ nm}^2$  and obtained results in agreement with cross sections of  $17 \times 17 \text{ nm}^2$ , which indicate that the computational cell sizes are large enough that periodic boundary conditions do not play an artificial role in the behavior of the shocked material. Atomic interactions are treated using unit charge Coulomb interactions combined with Lennard-Jones interactions. These potentials are found to yield a lattice constant (5.64 Å) in agreement with the experimental value and to yield sound speeds that deviate from experimental measurements by 10%–20%.

These molecular dynamics simulations do not explicitly solve Maxwell's equations for the electric and magnetic fields. However, since the wavelength of radiation emitted at frequencies considered here (longer than  $10 \mu\text{m}$ ) is much longer than the dimensions of the computational cell, it is expected that the total polarization current generated in the computational cell will be closely related to the generated electromagnetic radiation for frequencies above the phonon frequencies (above about 10 THz in this NaCl model) where the material has good transmission properties. The shock propagation direction component of the total electric polarization current is  $J = \sum_i v_{z,i} q_i$  where  $q_i$  is the charge and  $v_{z,i}$  is the shock direction ( $z$ ) component of the velocity of atom  $i$ . Emission characteristics are discussed in detail below.

Figure 1 shows results of about 30 ps duration simulations of shocks propagating in the [111] and [100] directions initiated with piston velocities of 200 m/s. This relatively small piston velocity generates a shock that applies a uniaxial strain of 0.03–0.04 to the postshock material and increases the material temperature less than 1 K. Such strains are readily experimentally achievable (see, e.g., Ref. [4]). Figure 1 compares the shocked and unshocked Fourier transform of the shock propagation direction component of the total electric polarization current in the computational cell. Narrow peaks are observed in the shocked simulation that do not exist in the unshocked simulation. From the peak widths, the coherence length of the radiation emitted in vacuum is determined to be about 5 and 3 nm for the 16 THz, [111] peak, and 22 THz, [100] peak, respectively. These lengths are comparable to those of some commonly used lasers. The coherence times are nearly Fourier transform limited, suggesting that longer coherence lengths could be demonstrated by increasing the shock propagation time.

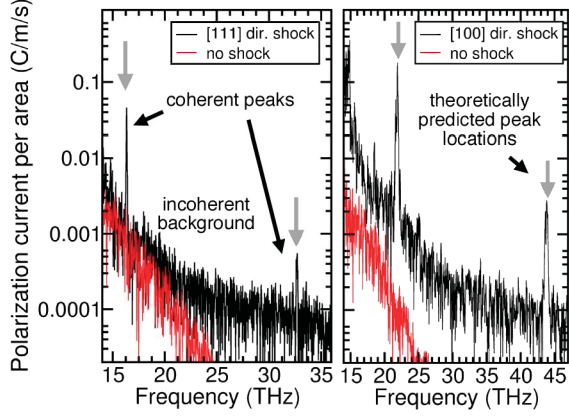


FIG. 1 (color). Fourier transform of the electric polarization surface current component in the shock propagation direction for molecular dynamics simulations of a shock propagating through NaCl in the [111] direction (left) and [100] direction (right). Narrow bandwidth, coherent peaks exist in the shocked simulations (black) that do not exist in the simulations without shocks. Gray arrows are emission frequencies predicted by Eq. (3). The coherence length for emission from the 16 THz peak in the [111] case is about 5 mm, comparable to that of some commonly used lasers. Thermal noise gives rise to an incoherent background.

Equation (3) predicts that emission should occur in multiples of 5.4 THz in the [111] case since the periodic unit for the [111] direction in NaCl  $a = 9.78 \text{ \AA}$  and the shock speed observed in the simulation is  $v_s = 5300 \text{ m/s}$ . The 16 and 32 THz peaks on the left of Fig. 1 correspond to 3 and 6 times the fundamental frequency of 5.4 THz [ $\ell = 3$  and 6 in Eq. (3)], in excellent agreement with theory (gray arrows). The 16 THz peak can be attributed to structure within the unit cell of distance  $a = 3.26 \text{ \AA}$  [i.e.,  $\ell = 1$  if  $a = 3.26$  in Eq. (3)], which is the distance between atomic lattice planes of like charge in the [111] direction (the NaCl crystal consists of alternating planes of positively and negatively charged atoms in the [111] direction). Lattice planes are compressed as the shock propagates through the crystal, generating an alternating polarization current with a frequency associated with the rate at which the shock propagates through the lattice planes. If the shock speed is constant, the generated frequencies are constant and the coherence time of the emitted radiation is expected to be proportional to the time duration of the propagation of the shock wave. Equation (3) is also in good agreement with the [100] direction data where  $a = 5.64 \text{ \AA}$  and the observed shock speed is  $v_s = 6200 \text{ m/s}$  with peaks corresponding to the  $\ell = 2$  and 4 cases. These peaks correspond to the distance between neighboring lattice planes in the crystal.

The molecular dynamics simulations enable simulation of experimentally accessible lengths of material in the shock propagation direction, but the area of shock fronts in typical experiments is much larger than can be simulated, typically ranging from  $\mu\text{m}$  to cm diameter. Deviations of the shock front from perfect planarity on

these length scales are experimentally inevitable, and we show that such deviations can affect emission characteristics. The electric field emitted from a nonplanar shock front in the far-field limit, far from the shock front can be calculated using polarization current magnitude data from the infinitely planar shock molecular dynamics simulations as an integral over polarization current at the shock front,

$$|E(\vec{r})|^2 = \left( \frac{\mu_0 \omega}{4\pi} \frac{\sin(\theta)}{|r|} \right)^2 \left| \int_{\text{shock}} d\vec{r}' j(\vec{r}') e^{i\omega[t - (|\vec{r} - \vec{r}'|/c)]} \right|^2, \quad (4)$$

where  $j$  is the  $\omega$  frequency component of the polarization current on the shock front surface (oriented normal to the shock front, as in Fig. 1) and  $\theta$  is the angle between  $\vec{r}$  and a vector normal to the shock front. The integral is over the shock front, taken to be in the  $x$ - $y$  plane. The integral in Eq. (4) can be written in terms of the Fourier transform of  $j$  as  $|\tilde{j}(k_x = \frac{\omega}{c} \sin\theta, k_y = 0)|^2$  when  $\vec{r}$  lies in the  $x$ - $z$  plane. The polarization current is well described by  $j(\vec{r}') = j_0 e^{i\omega z(\vec{r}')/v_s}$  where  $j_0$  is the magnitude of the  $\omega$  component of the polarization current obtained from MD simulations of planar shocks and  $z(\vec{r}')$  describes the position of the shock front in the propagation direction as a function of location on the front surface  $\vec{r}'$ . The phase of  $j$  (but not the magnitude) depends very sensitively on the position of the shock front  $z$ , to variations of a few angstroms in the case of NaCl ( $2\pi \frac{v_s}{\omega}$  is on the order of angstroms). Therefore the distribution and intensity of the emitted radiation (but not the coherence length) will depend very sensitively on the atomic-scale shape of the shock front, and can potentially be used as an atomic-scale probe of its shape.

Extremely flat shock fronts with root-mean-square variation in position of 0.7 nm over a  $75 \mu\text{m}$  diameter shock front have been measured in laser-driven shocks [3]. Deviations from perfect planarity can result from nonplanar drive mechanisms (spatially nonuniform drive beam or piston, etc.) and crystal defects and imperfections. To calculate the emission characteristics including such deviations from perfect planarity, we consider the case where the shock front surface  $z(\vec{r}')$  possesses spatial fluctuations with wave vectors less than a specified maximum,  $k_{\text{max}}$ ; i.e., let  $\tilde{j}(\vec{k}) = \frac{\pi^2}{k_{\text{max}}^2} \sum_{\vec{r}'} j_0 e^{i(\omega/v_s)z(\vec{r}')} e^{-i\vec{k}\vec{r}'}$  where  $\vec{r}' = (m \frac{\pi}{k_{\text{max}}}, n \frac{\pi}{k_{\text{max}}})$ , where  $m$  and  $n$  are integers such that  $0 \leq m, n < \frac{\sqrt{A} k_{\text{max}}}{\pi}$  for a square shock front and  $\frac{\omega}{c} \sin(\theta) \leq k_{\text{max}}$ . Here,  $A$  is the shock front area and  $k_{\text{max}}$  is a disorder parameter related to the density of crystal defects or degree of spatial uniformity of the source driving the shock, etc. Since precise control over the planarity of the shock over large areas may be challenging to achieve, we consider random fluctuations in the shock front surface by taking  $\frac{\omega}{v_s} z(\vec{r}')$  to be a random variable with value between 0 and  $2\pi$  for each value of  $\vec{r}'$ . The electric field expectation is

$$\langle |E(\vec{r})|^2 \rangle = \left( \frac{\mu_0 \omega}{4} \frac{\sin(\theta)}{|r|} \right)^2 \frac{A}{k_{\text{max}}^2} |j_0|^2, \quad (5)$$

which has a distribution similar to that of an oscillating dipole with polarization normal to the shock front. The corresponding power radiated in all directions is given by

$$\langle p \rangle = \frac{\pi \mu_0 \omega^2}{12c} \frac{A}{k_{\max}^2} |j_0|^2. \quad (6)$$

In the case of the 22 THz peak in the right side of Fig. 1 where  $j_0 = 0.18$  C/m/s, for shock front area  $A = 1$  cm<sup>2</sup> and  $2\pi/k_{\max} = 5 \times 10^{-6}$  m, Eq. (6) predicts the shock coherently radiates with a readily detectable power of  $4 \times 10^{-5}$  W while it propagates. The random shock front case is a worst case scenario: if systems with  $k_{\max} \ll \frac{\omega}{c}$  can be achieved (plausible given current state of the art), then the emission can be directed and can have substantially higher emission power that scales with  $A^2$ . The energy conversion efficiency for generation of this radiation is likely to be extremely small since far more energy is required to physically compress the material than to produce the radiation.

The emission peaks studied in this work have frequencies that are up to 2 times higher than phonon frequencies. Observation of these peaks requires that there be spectral components of atom velocities at these higher frequencies around the shock front. Such high frequency components of atomic motion can be generated only if the shock front (or part of it) is very sharp. The natural shock front rise distances in the molecular dynamics simulations are several lattice planes. This effect represents a mechanism through which elastic shock wave rise times can potentially be experimentally measured; to our knowledge, such a measurement has never been made.

Narrow bandwidth radiation in the terahertz frequency regime like that generated in the shocked crystal is useful and has proven to be challenging to generate. Such generation is currently an area of active research [9]. Uses for terahertz radiation range from fundamental studies of phonon dynamics to new methods of medical and biological imaging to security screening devices able to penetrate clothing to detect explosives or other weapons [10,11].

*Concluding remarks.*—Suspected nonequilibrium (non-thermal) optical radiation in the visible regime has been observed from shocked dielectrics under some conditions [12–15], but this radiation appears to have a different origin than the coherent emission discussed here that occurs in a different part of the electromagnetic spectrum and results from the crystallinity of the lattice.

For the computational cell size used in Fig. 1, we find that the lower frequency coherent peak is observed above the background at 25 K but not at 77 K for shocks in the [100] direction. We expect that the area of the shock and propagation duration will affect the relative amplitudes of the coherent peaks and the background since these two amplitudes scale differently with these quantities. Therefore, we speculate that it may be possible to observe the coherent emission at higher temperatures under some conditions [6].

We note that it is well known that coherent radiation at almost any frequency can be obtained from a *coherent* source using materials with a nonlinear optical response. This approach utilizes radiation from a coherent source to generate new coherent radiation. The coherent radiation mechanism presented in this work is fundamentally distinct from such nonlinear approaches in that coherence results from the crystal lattice rather than another coherent source. The optical nonlinearity mechanism works in amorphous materials while the shocked crystal mechanism does not.

We thank E. Ippen and F. Kaertner of MIT, J. Glowina, A. Taylor, and R. Averitt of LANL, and L. Fried and D. Hicks of LLNL for helpful discussions. This work was supported in part by the Materials Research Science and Engineering Center program of the National Science Foundation under Grant No. DMR-9400334. This work was performed in part under the auspices of the U.S. Department of Energy by University of California, Lawrence Livermore National Laboratory, under Contract No. W-7405-Eng-48.

---

\*Electronic address: reed23@llnl.gov

- [1] A. M. Sessler and D. Vaughan, *Am. Sci.* **75**, 34 (1987).
- [2] A. H. Jones, W. M. Isbell, and C. J. Maiden, *J. Appl. Phys.* **37**, 3493 (1966).
- [3] D. S. Moore, K. T. Gahagan, J. H. Reho, D. J. Funk, S. J. Buelow, and R. L. Rabie, *Appl. Phys. Lett.* **78**, 40 (2001).
- [4] E. Zaretsky, *J. Appl. Phys.* **93**, 2496 (2003); F. Muller and E. Schulte, *Z. Naturforsch., A: Phys. Sci.* **33**, 918 (1978); W. J. Murri and G. D. Anderson, *J. Appl. Phys.* **41**, 3521 (1970).
- [5] C. Kittel, *Introduction to Solid State Physics* (John Wiley and Sons, New York, NY, 1996).
- [6] E. J. Reed, M. Soljačić, and J. D. Joannopoulos (to be published).
- [7] M. O. Scully and M. S. Zubairy, *Quantum Optics* (Cambridge University Press, Cambridge, U.K., 1997).
- [8] E. M. Bringa, J. U. Cazamias, P. Erhart, J. Stolken, N. Tanushev, B. D. Wirth, R. E. Rudd, and M. J. Caturla, *J. Appl. Phys.* **96**, 3793 (2004).
- [9] P. H. Siegel, *IEEE Trans. Microw. Theory Tech.* **50**, 910 (2002).
- [10] P. H. Siegel and R. J. Dengler, *Proc. SPIE-Int. Soc. Opt. Eng.* **5354**, 1 (2004).
- [11] M. C. Kemp, P. F. Taday, B. E. Cole, J. A. Cluff, A. J. Fitzgerald, and W. R. Tribe, *Proc. SPIE-Int. Soc. Opt. Eng.* **5070**, 44 (2003).
- [12] S. B. Kormer, *Usp. Fiz. Nauk* **68**, 641 (1968).
- [13] T. Ahrens, G. Lyzenga, and A. C. Mitchell, in *High Pressure Research in Geophysics* (Manghani Center for Academic Publication, Japan, 1982), p. 579.
- [14] K. Kondo and T. Ahrens, *Phys. Chem. Miner.* **9**, 173 (1983).
- [15] D. Schmitt, B. Svendsen, and T. Ahrens, in *Shock Waves in Condensed Matter* (Plenum Press, New York, 1986), p. 286.